2022 44th Annual International Conference of
the IEEE Engineering in Medicine & Biology Society (EMBC)
Scottish Event Campus, Glasgow, UK, July 11-15, 2022

2022 44th Annual International Conference of the IEEE Engineering in Medicine & Biology Society (EMBC) | 978-1-7281-2782-8/22/$31.00 ©2022 IEEE | DOI: 10.1109/EMBC48229.2022.9871323

Temporal and morphological characteristics of high-frequency oscillations in an acute in vivo model of epilepsy

Sophia R. Zhai, Daniel Ehrens, Adam Li, Fadi Assaf, Yitzhak Schiller, Sridevi V. Sarma, and Rachel June Smith, *Member, IEEE*

Abstract— **Approximately 30% of patients with epilepsy do not respond to anti-epileptogenic drugs. Surgical removal of the epileptogenic zone (EZ), the brain regions where the seizures originate and spread, can be a possible therapy for these patients, but localizing the EZ is challenging due to a variety of clinical factors. High-frequency oscillations (HFOs) in intracranial electroencephalography (EEG) are a promising biomarker of the EZ, but it is currently unknown whether HFO rates and HFO morphology modulate as pathological brain networks evolve in a way that gives rise to seizures. To address this question, we assessed the temporal evolution of the duration of HFO events, amplitude of HFO events, and rates of HFOs per minute. HFO events were quantified using the 4AP *in vivo* rodent model of epilepsy, inducing seizures in two different brain areas. We found that the duration and amplitude of HFO events were significantly increased for the cortex model when compared to the hippocampus model. Additionally, the duration and amplitude increased significantly between baseline and pre-ictal HFOs in both models. On the other hand, the two models did not display a consistent increasing or decreasing trend in amplitude, duration or rate when comparing ictal and postictal intervals.**

Clinical Relevance— **We assessed the amplitude, duration, and rate of HFOs in two acute *in vivo* rodent models of epilepsy. The significant modulation of HFO morphology from baseline to pre-ictal periods suggests that these features may be a robust biomarker for pathological tissue involved in epileptogenesis. Moreover, the differences in HFO morphology observed between cortex and hippocampus animal models possibly indicate that different structural network characteristics of the EZ cause this modulation. In all, we found that HFO features modulate significantly with the onset of seizures, further highlighting the need to consider of HFO morphology in EZ-localizing studies.**

I. Introduction

Medically refractory epilepsy (MRE) is a severe neurological disorder that affects over 20 million people around the world [1], [2]. Frequent hospitalization and epilepsy-related disabilities greatly impact the lives of MRE patients [3]. For focal MRE patients (approximately 50% of MRE patients), the epileptogenic zone (EZ)—a hypothetical region in the brain composed of and connected to a large-scale neuronal network —is the source of the seizures. Identifying the EZ accurately and reliably is critical for the success of treatment by means of resection of the EZ. HFOs have been shown to be a promising biomarker of epileptogenic tissue that may help clinicians identify the EZ and thus improve success rates after surgical resection [4]–[6].

HFOs are transient events that are present both physiologically and pathologically [7]. They are often classified into two subgroups based on their frequency content, ripples (80-250 Hz) and fast ripples (250-500 Hz) [8]. Although it has been shown that HFOs are correlated with already pathological tissue, it is still not clear how HFOs modulate during the process of seizure genesis. Various rodent models of epilepsy are utilized to understand different mechanisms that underlie the genesis of seizures [9]–[12]. Thus, we implemented an acute model of epilepsy in two different brain areas (S1 cortex and hippocampus) to examine the modulation of HFO features throughout the process of seizure genesis.

II. Methodology

A. Animal Models

All experiments were approved by the Technion Institutional Animal Ethics Committee. Six adult male wildtype 8-14 week old Wistar rats were used (230-430 gr) to acquire electrophysiological recordings during non-survival experiments. Electrographical seizures were induced through the local application of 4-aminopyridine (4AP). 4AP was applied at two different brain sites: S1 barrel cortex (as in [12]), and CA3 of the posterior hippocampus (AP -5.8, ML 4.6, DV 5.5).

B. Electrophysiological Recordings

Local field potential (LFP) recordings were acquired using two different electrode probes fabricated by NeuroNexus (Ann Arbor, MI). For the hippocampus model, a custom-designed rDBSA probe with 11 recording channels was used, the schematic and stereotaxic implantation map is shown in

*Research supported by . RJS is supported by an NIH IRACDA grant (ASPIRE at JHU). DE is supported by the Howard Hughes Medical Institute through the James H. Gilliam Fellowships for Advanced Study program. AL is supported by the NSF GRFP, Whitaker Fellowship and the Chateaubriand Fellowship. SVS is supported by NIH R21 NS103113.

S.R.Z. , R.J.S., D.E., A.L., and S.V.S. are with the Department of Biomedical Engineering, Johns Hopkins University, Baltimore, MD 21224 USA

F.A. and Y.S. are with the Rappaport Faculty of Medicine and Research Institute, Technion - Israel Institute of Technology, Haifa, Israel.

Correspondence should be addressed to Sophia R. Zhai, Department of Biomedical Engineering, Johns Hopkins University. Phone: 720-609-6497; e-mail: srzhai01@gmail.com).

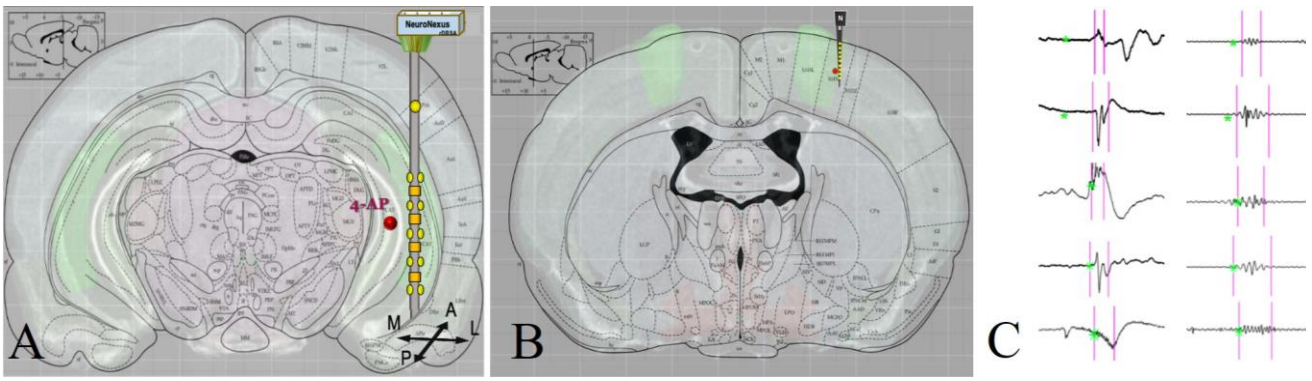

Figure 1. Electrode design and stereotaxic implantation map of (A) the hippocampus model and (B) cortex model. (C) Several common morphologies of HFOs, with the left side displaying the raw data recorded by a contact, and the right side plotting the filtered data. The two magenta lines indicate the start and stop times of the HFO event.

Fig. 1A. For the cortex model, a linear array with 16 channels was used (A1x16-5mm-50-177) to record from all six layers of the S1 barrel cortex, shown in Fig.1B.

LFP signals were pre-amplified and then digitized by a 32-channel AlphaLab SnR (Alpha Omega, Nazareth, Israel) system at a sampling frequency of 11 kHz. The LFP was notch filtered at 50 Hz and referenced to a ground wire on the surface of the cortex distant from the recording site. Channel numbering increased from the most dorsal contact on the electrode probe towards the most ventral contact.

C. *HFO Detection*

Visual identification of HFOs is time-consuming and highly subjective [13]. Thus, automatic detection of HFOs removes some of the viewer bias and allows for a more rapid investigation of these neural events. The RMS detector developed by Staba et. al 2002 was utilized and parameters were determined for the various models by visual inspection of HFO detections [14]. We first applied a least-squares linear-phase FIR filter (passband 100-500 Hz) to the raw data. Subsequently, we calculated the mean root mean square within a 3 ms sliding window. An event was then determined to be a candidate HFO if the root mean square was more than 5 times the standard deviations above the mean RMS value and was longer than 6 ms. Events less than 10 ms apart were identified as a single event. Candidate HFO events with more than six peaks that had a root mean square more than 3 standard deviations above the mean were recorded as final HFO events.

D. *Calculation of HFO Features*

A computational analysis of the temporal structure of the HFO duration and amplitude and computation of HFO rate was performed for three animals of each model.

Four time intervals were considered. Firstly, the baseline period consisted of 10 minutes of healthy-baseline recording, prior to the application of 4AP. The pre-ictal period was identified as the period of time after injection but before the first seizure occurred. The ictal period was defined as the first electrographical seizure from onset to termination. Seizure onset markings were identified by a certified epileptologist (Y.S.). Finally, the post-ictal period was defined to be the time interval from the first seizure offset to the next seizure onset. This state is the most comparable to human inter-ictal data.

HFO rate was calculated as the number of events detected in 1-minute windows with 50% overlap. To compare rates across time periods and between models, one rate was calculated for each time interval in detections per minute. Then the rates were averaged for each time interval for all animals in each model. Amplitude was measured as the absolute value of the maximum prominence of the peaks within a detection. Duration was calculated as the difference between the end time and start time of the detected event.

III. RESULTS

A. *Longer, high-amplitude HFO events in cortex model*

Though we used the same detector parameters in both models, we found different magnitudes of rate, duration, and amplitude between the two models. However, we found that they exhibited similar trends through the process of seizure genesis.

We detected more HFOs in the cortex model than the hippocampus model (see representative examples, Fig. 2). Additionally, the durations of HFOs in the cortex model were significantly greater than the durations of HFOs in the hippocampus model for each of the four time periods (Mann-Whitney U test, $p<0.05$, Fig. 3A). Similarly, the amplitudes of HFOs in the cortex model were significantly higher than HFO amplitudes in the hippocampus model of the same time interval (Mann-Whitney U test, $p<0.05$, Fig. 3B). For each of the eight groups considered in Fig. 3A and Fig. 3B, the total number of observations are: n = 2056, 753, 728, 465, 3303, 26985, 3107, 8418 respectively.

B. *HFOs modulate from baseline to pre-ictal state*

In the hippocampus model, the ictal HFOs had longer durations than baseline, and pre- and post-ictal HFOs (Mann-Whitney U test, $p<0.05$, Fig. 3A). In contrast, the durations of the ictal cortex model was comparable to that of the baseline HFOs, and pre-ictal and post-ictal HFO durations were comparable as well. However, the pre-ictal and post-ictal cortex HFO durations were significantly longer than that of the baseline and ictal events (Mann-Whitney U test, $p<0.05$, Fig. 3A). The amplitude was significantly higher for the ictal and post-ictal HFOs than the pre-ictal which was significantly

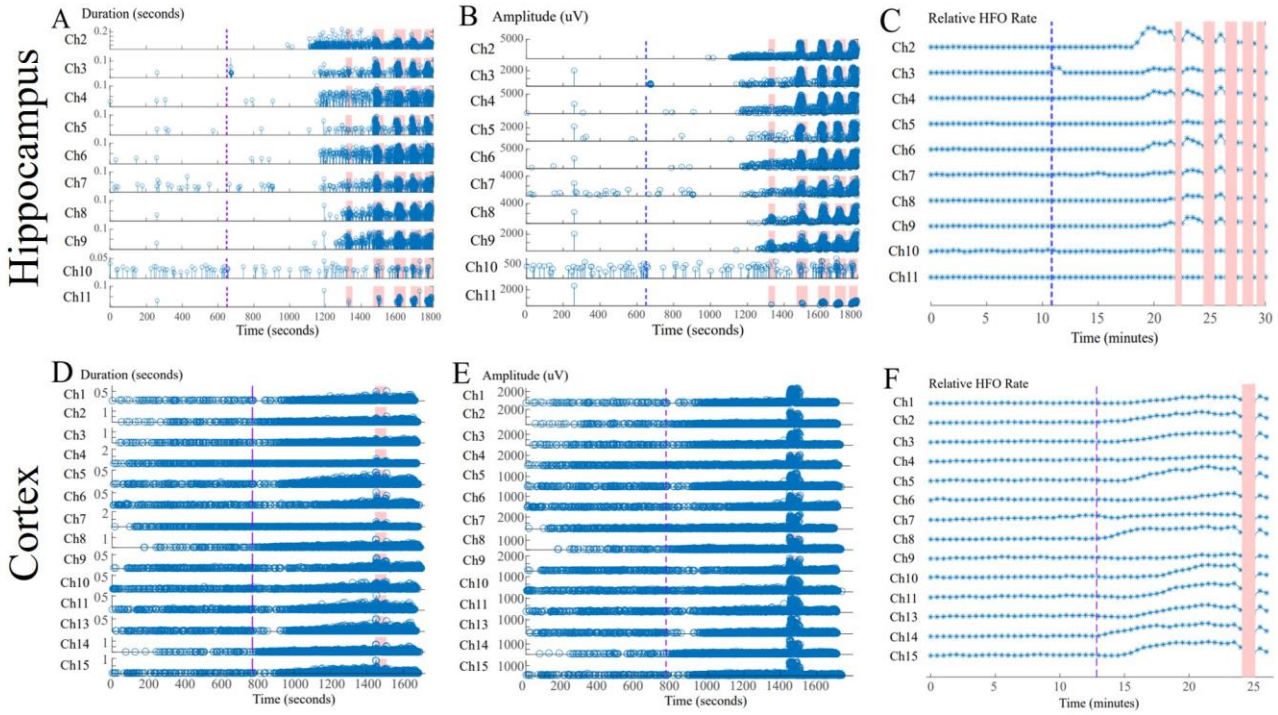

Figure 2. Representative HFO events and temporal evolution of seizure genesis characteristics in representative animals from the hippocampus and cortex models. Duration and amplitude were both plotted in a stem plot to allow for visualization of temporal changes in duration and amplitude while taking into consideration the overall number of the detections. The start of the injection period is marked by the purple line, while the red intervals represent the marked seizures from the in vivo experiments. Stem plots of the (A) duration and (B) amplitude of HFOs for each of the included channels in the hippocampus model. (C) The rate of HFOs in detections per minute in the hippocampus model is plotted for each of the channels (Channel 1 was removed as it was marked as a noisy/bad channel during recording). The relative HFO rates did not include the events during seizures so as not to skew the distribution disproportionately. The duration, amplitude, and rate of HFO events in a representative cortex animal is plotted in the same manner in panels (D) (E) and (F), respectively, with Channel 12 removed as a noisy/bad channel.

larger than the baseline amplitudes for the hippocampus animals. For the cortex model, the pre-ictal amplitudes were the largest. The post-ictal amplitudes were significantly lower than the pre-ictal but higher than the baseline amplitude of HFOs. Interestingly, the ictal amplitudes were the smallest in the cortex model (Mann-Whitney U test, $p<0.05$, Fig. 3B). Lastly, HFO rates increased significantly from baseline to pre-ictal intervals in the cortex model (Mann-Whitney U test, $p<0.05$, Fig. 3C). It is important to note that the post-ictal period in these models were also pre-ictal periods for the subsequent seizure that often began soon after the first seizure terminated.

C. HFO features vary spatially

HFO rates varied spatially between channels in the process of seizure genesis, indicating not only a temporal variance in

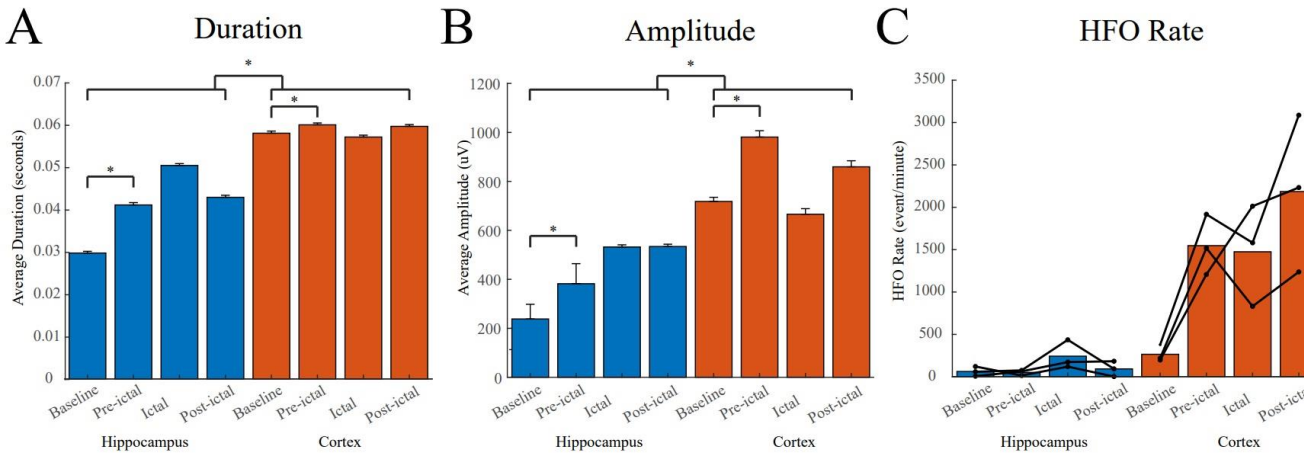

Figure 3. Significant variation of rate, duration, and amplitude for the four time periods of the seizure genesis process and between the two *in vivo* animal models. The four major time periods relevant to seizure genesis include: (1: baseline/pre-injection, 2: pre-ictal, 3: ictal, and 4: postictal). The median duration (A) and amplitude (B) of all detected events during the four time intervals are plotted as bar graphs. (C) A bar graph comparing HFO rates of the two epileptogenesis models during the four time periods. The average HFO rate and trajectory of rate across time periods for individual animals is shown as the line across the bar graph. The bar value reflects the mean value of the three animals.

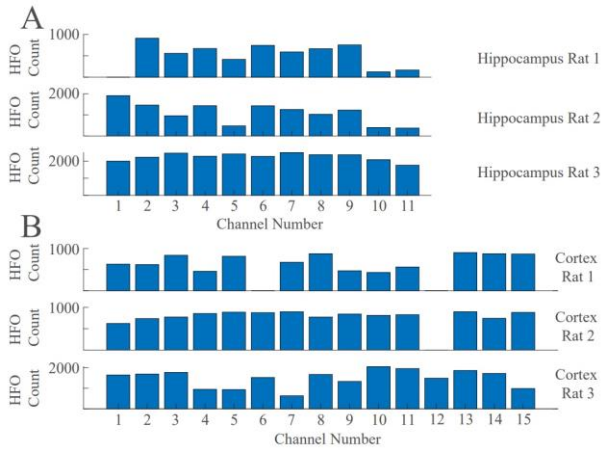

Figure 4. Total number of HFOs are plotted for each of the animals included in the (A) hippocampus and (B) cortex models. The channels are labeled from the most dorsal (1) to the most ventral (11 or 15 for hippocampus and cortex model, respectively). The toxin was injected around channel 5 in the hippocampus model.

HFOs but also a spatial variance between epileptogenic tissue (Fig. 4). The hippocampus model exhibits the trend where channels 2-4 and 6-9 seem elevated in comparison to the other channels. The injection site, and thus the hypothesized EZ, is closest to channel 5 at a dorsal-ventral level but may be slightly more lateral. In the cortex model, channels 1-3 and 13-15 appear elevated generally. For the cortex model, the most dorsal channels represent layer 2 or 3 and the more ventral channels are layer 5 and layer 6 of the cortex. Thus, the number of total HFO events were higher in the regions that were closer to the toxin injection sites in the hippocampus model.

IV. Discussion

HFO morphology varied greatly between the two 4AP models of epilepsy (Fig. 2 and 3). The characteristics of HFOs demonstrated similar trends consistently between the two different *in vivo* models of epilepsy while having significantly different magnitudes in all four time intervals. In general, we detected a greater number of HFOs in the cortex model when compared to the hippocampus model. The rate, duration, and amplitude of HFO events varied temporally for animals throughout the process of epileptogenesis, with dramatic increases in rate of HFOs compared to baseline after injection of 4AP for both the hippocampus model and the cortex model. Due to the large number of observations, the statistical significance of these differences is robust. This corroborates previous research which demonstrated that HFOs may correspond to epileptogenic tissue [4], [5] because more HFOs were detected as the brain network moved toward seizure onset. The characteristics of duration and amplitude also exhibited significant changes throughout seizure genesis. The amplitude and duration of HFOs both generally increased with the pathological state, most robustly in the hippocampus model. Additionally, the spatial variance between features of HFOs suggest that the localizing aspects of high-frequency activity may hold during the genesis of seizures (Fig. 4).

V. Conclusion

HFO features evolve throughout seizure onset as brain networks pathologically evolve and do so differently in two different animal models of epileptogenesis. These characteristics should be accounted for in more fine-grained detection of high-frequency events. Duration and amplitude of seizures increase for both models and may be a robust biomarker for epileptogenesis while other characteristics may need to be investigated during seizure. However, these three characteristics may have varying absolute magnitudes in different animal models indicating that they also may have the potential to differentiate mechanisms of actions in seizure genesis.

Acknowledgment

The authors would like to thank Dr. Jackie Schiller for invaluable support and advice. Also, we thank Fadi Aeed and Yara Otor for experimental training and support.

References

[1] A. K. Ngugi, S. M. Kariuki, C. Bottomley, I. Kleinschmidt, J. W. Sander, and C. R. Newton, "Incidence of epilepsy: a systematic review and meta-analysis.," *Neurology*, vol. 77, no. 10, pp. 1005–1012, 2011.

[2] B. C. Jobst, "Consensus Over Individualism: Validation of the ILAE Definition for Drug Resistant Epilepsy," *Epilepsy Curr.*, vol. 15, no. 4, pp. 172–173, 2015.

[3] M. I. Murray, M. T. Halpern, and I. E. Leppik, "Cost of refractory epilepsy in adults in the USA," *Epilepsy Res.*, vol. 23, no. 2, pp. 139–148, 1996.

[4] J. Jacobs, P. Levan, C. D. Chtillon, A. Olivier, F. Dubeau, and J. Gotman, "High frequency oscillations in intracranial EEGs mark epileptogenicity rather than lesion type," *Brain*, vol. 132, no. Pt 4, pp. 1022–1037, 2009.

[5] B. Frauscher *et al.*, "High-frequency oscillations: The state of clinical research," *Epilepsia*, vol. 58, no. 8, p. 1316, 2017.

[6] K. Charupanit, I. Sen-Gupta, J. J. Lin, and B. A. Lopour, "Detection of anomalous high-frequency events in human intracranial EEG," *Epilepsia Open*, vol. 5, no. 2, p. 263, 2020.

[7] M. T. Kucewicz *et al.*, "High frequency oscillations are associated with cognitive processing in human recognition memory," *Brain*, vol. 137, no. Pt 8, pp. 2231–2244, 2014.

[8] M. Zijlmans, P. Jiruska, R. Zelmann, F. S. S. Leijten, J. G. R. Jefferys, and J. Gotman, "High-frequency oscillations as a new biomarker in epilepsy," *Ann. Neurol.*, vol. 71, no. 2, pp. 169–178, 2012.

[9] W. C. Chang *et al.*, "Loss of neuronal network resilience precedes seizures and determines the ictogenic nature of interictal synaptic perturbations," *Nat. Neurosci.*, vol. 21, no. 12, pp. 1742–1752, 2018.

[10] A. Cymerblit-Sabba and Y. Schiller, "Development of hypersynchrony in the cortical network during chemoconvulsant-induced epileptic seizures in vivo.," *J. Neurophysiol.*, vol. 107, no. 6, pp. 1718–1730, 2012.

[11] A. Cymerblit-Sabba and Y. Schiller, "Network dynamics during development of pharmacologically induced epileptic seizures in rats in vivo.," *J. Neurosci.*, vol. 30, no. 5, pp. 1619–1630, 2010.

[12] F. Aeed, T. Shnitzer, R. Talmon, and Y. Schiller, "Layer- and Cell-Specific Recruitment Dynamics during Epileptic Seizures In Vivo," *Ann. Neurol.*, vol. 87, no. 1, pp. 97–115, 2020.

[13] A. M. Spring *et al.*, "Interrater reliability of visually evaluated high frequency oscillations," *Clin. Neurophysiol.*, vol. 128, no. 3, pp. 433–441, 2017.

[14] R. J. Staba, C. L. Wilson, A. Bragin, and I. Fried, "Quantitative analysis of high-frequency oscillations (80-500 Hz) recorded in human epileptic hippocampus and entorhinal cortex," *J. Neurophysiol.*, vol. 88, no. 4, pp. 1743–1752, 2002.